Eur. Phys. J. B **53**, 509–515 (2006)
DOI: 10.1140/epjb/e2006-00402-8

THE EUROPEAN PHYSICAL JOURNAL B

Pattern formation in reaction-diffusion system in crossed electric and magnetic fields

S.S. Riaz[1], S. Banarjee[2], S. Kar[1], and D.S. Ray[1,a]

[1] Indian Association for the Cultivation of Science, Jadavpur, Kolkata 700 032, India
[2] Department of Physics, Indian Institute of Science, Bangalore 560012, India

Received 27 July 2006
Published online 6 November 2006 –

Abstract. We consider a reaction-diffusion system in crossed electric and magnetic fields lying on the reaction plane. It is shown that a charge separation along the direction normal to the reaction plane resulting in a diffusional flux may cause a differential flow induced chemical instability and stationary pattern formation on a homogeneous steady state. This pattern is generically different from a Turing pattern modified by the crossed fields. The special role of magnetic field is emphasized. Our theoretical analysis is corroborated by numerical simulation on a reaction-diffusion system in three dimensions.

PACS. 82.40.Ck Pattern formation in reactions with diffusion, flow and heat transfer – 47.54.-r Pattern selection; pattern formation – 05.45.-a Nonlinear dynamics and chaos

1 Introduction

The spontaneous formation of structure in spatially extended systems under far-from-equilibrium condition is an active area of wide current interest [1,2]. The subject has got its early impetus from the discovery of Turing instability or diffusion-driven instability in an homogeneous reaction-diffusion system [3] and has grown in various directions over the decades. An important endeavor in this development is how the oscillations, wave propagation and patterns are affected by external fields. It has been demonstrated that applying electric fields can have a profound effect on the propagation of waves in ionic chemical reactions, e.g., by causing wave splitting, acceleration or deceleration with effect of annihilation, production of spirals from target patterns etc. [4–6]. A constant external electric field may also generate a differential flow induced stationary pattern or destabilize it under appropriate conditions [10–12]. The possibility of using electric field as a control parameter for reaction front instabilities has been examined [7]. It has been shown [8] that by applying constant electric field separating the reactant anions and autocatalyst cations, lateral instabilities can be induced while planner fronts can be stabilized with electric field in the opposite orientation. A close look into these studies suggests that consideration of a small but finite extension of the two-dimensional reaction plane along its normal direction and the electric field-induced drift current of ions may lead to the development of interesting cross effect when a constant magnetic field is allowed to interact in an appropriate geometry. The object of the present paper is to explore such a cross effect in a reaction-diffusion system in three dimensions. In what follows we show that when the crossed electric and magnetic fields are applied, a charge separation along the direction normal to the reaction plane containing the mutually perpendicular fields, resulting in a diffusional flux may cause differential flow induced chemical instability. This leads to stationary pattern formation on a homogeneous stable state.

Although it is well-known that magnetic field can significantly affect a number of chemical reactions which include, for example, geminate radical pair recombination [13–15], auto-oxidation of benzaldehyde by oxygen catalysed by Co(II) ions [16–18], the conspicuous feature of these work is the paramagnetic nature of the key reacting species. Several living systems are also susceptible to the variation of magnetic field. Furthermore, the effect of constant electric and strong magnetic field has been investigated [9] in BZ reaction. The present work represents how a magnetic field can induce pattern due to differential flow in a reaction-diffusion system even when the reacting species are not paramagnetic, which is to the best of our knowledge has not been investigated before. Second, this differential flow induced pattern not only appears for a critical range of magnetic field strength, but also vanishes beyond a spatial extension normal to the reaction plane along which the charge separation occurs. Third, we carry out our

[a] e-mail: pcdsr@mahendra.iacs.res.in

theoretical analysis and numerical simulation on a prototype reaction-diffusion system (chlorite-iodide-malonic acid (CIMA)) in three dimensions, which is the most well-studied system studied to date for the investigation of pattern formation and related issues from experimental point of view [19].

The outline of the paper is as follows: we introduce in Section 2 the basic equations for a reaction-diffusion system in presence of crossed electric and magnetic fields in a Hall type arrangement. In Section 3 we show how a differential flow induced instability can be realized by appropriate manipulation of the fields with help of linear stability analysis. The numerical simulation on pattern formation has been carried out in Section 4. The paper is concluded in Section 5.

2 Reaction-diffusion system in crossed fields

We consider a reaction-diffusion system in three dimensions in presence of crossed electric and magnetic fields,

$$u_t + \overrightarrow{\bigtriangledown}.\overrightarrow{j_u} = f(u,v) \tag{1}$$

$$v_t + \overrightarrow{\bigtriangledown}.\overrightarrow{j_v} = g(u,v). \tag{2}$$

Here $u(x,y,z,t)$ and $v(x,y,z,t)$ are the concentrations of the activator and inhibitor species, respectively. $f(u,v)$ and $g(u,v)$ are the reaction terms describing the kinetics. j_i $(i = u, v)$ is the flux of concentration of the ith species c_i $(i = u, v)$ and is comprised of two terms which are due to spatial diffusion and applied field of forces as follows;

$$\overrightarrow{j_i} = -D_i \overrightarrow{\bigtriangledown} c_i - m_i \overrightarrow{F_i} c_i \tag{3}$$

D_i is the diffusion coefficient of the ith species and m_i is given by $m_i = D_i/kT$, where k and T are the Boltzmann constant and temperature, respectively. The Lorentz force experienced by the ith ionic species with velocity v_i and charge $z_i|e|$ due to the electric field $\overrightarrow{E}$ and the magnetic field $\overrightarrow{B}$ is given by $\overrightarrow{F_i} = z_i|e|(\overrightarrow{E} + \overrightarrow{v_i} \times \overrightarrow{B})$. The divergence of concentration flux therefore yields

$$\overrightarrow{\bigtriangledown}.\overrightarrow{j} = -D \bigtriangledown^2 c_i - z_i|e|(D_i/kT)\overrightarrow{\bigtriangledown}.(\overrightarrow{E} + \overrightarrow{v_i} \times \overrightarrow{B})c_i. \tag{4}$$

To proceed further we first assume that the constant electric field is weak and generates a steady electric current $\overrightarrow{J}$ so that the displacement current term can be neglected from Maxwell's equation to obtain $\overrightarrow{\bigtriangledown} \times \overrightarrow{B} = \mu \overrightarrow{J}$, μ being the permeability of the medium. Since by Ohm's law we have $\overrightarrow{J} = \sigma_e(\overrightarrow{E} + \overrightarrow{v} \times \overrightarrow{B})$ and $\overrightarrow{\bigtriangledown}.\overrightarrow{\bigtriangledown} \times \overrightarrow{B} = 0$ where σ_e refers to electrical conductivity, one obtains

$$\overrightarrow{\bigtriangledown}.\overrightarrow{J} = \sigma_e \overrightarrow{\bigtriangledown}.(\overrightarrow{E} + \overrightarrow{v} \times \overrightarrow{B}) = 0. \tag{5}$$

Therefore from equations (4) and (5) we are led to the following equation:

$$\overrightarrow{\bigtriangledown}.\overrightarrow{j_i} = -D_i \bigtriangledown^2 c_i - z_i|e|(D_i/kT)(\overrightarrow{E} + \overrightarrow{v_i} \times \overrightarrow{B}).\overrightarrow{\bigtriangledown} c_i. \tag{6}$$

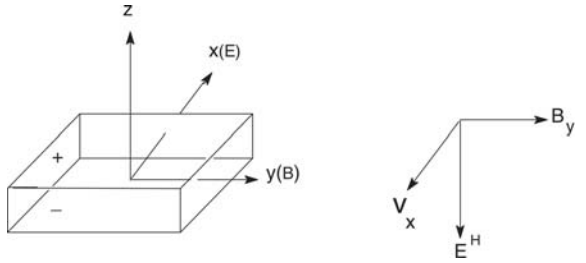

Fig. 1. The schematic experimental setup for the reaction-diffusion system in crossed fields.

We now consider a reaction [19,20] with negative ions only. An electric field is applied along x-direction to the reaction plane xy which has a finite but small extension along z direction. This causes a flow or drift current in the negative x-direction [11,12,21]. In addition a magnetic field B lying in the reaction plane points in the positive y-direction. As a result the Lorentz force acts to deflect the negative ions in the z-direction. Because of accumulation of opposite charges on both sides of the reaction plane, a Hall electric field E^H builds up in the Z-direction that balances the Lorentz force in the steady state and current flows only in the x-direction. The situation is depicted in Figure 1. Also the spatial extension of the xy reaction plane is assumed to be much larger compared to that in z-direction so that one may comprehend a differential flow along this direction. Thus the layer must be thick enough to allow the formation of spatial structure for a finite residence time of the reaction intermediate and a spatial extension of the order of a wavelength. In accordance with the condition for Hall effect we therefore assume that the velocity $\overrightarrow{v_i}$ of the ions is essentially due to the drift [22,23] because of the constant electric field so that by Einstein's relation we may use $\overrightarrow{v_i} = z_i|e|(D_i/kT)\overrightarrow{E}$. This implies we neglect altogether any effect due to diffusion current. We then arrive at the following two equations

$$u_t = f(u,v) + D_u \bigtriangledown^2 u + z_u|e|(D_u/kT)\overrightarrow{E}.\overrightarrow{\bigtriangledown} u + (z_u|e|D_u/kT)^2 \overrightarrow{E} \times \overrightarrow{B}.\overrightarrow{\bigtriangledown} u \tag{7}$$

$$v_t = g(u,v) + D_v \bigtriangledown^2 v + z_v|e|(D_v/kT)\overrightarrow{E}.\overrightarrow{\bigtriangledown} v + (z_v|e|D_v/kT)^2 \overrightarrow{E} \times \overrightarrow{B}.\overrightarrow{\bigtriangledown} v. \tag{8}$$

Equations (7, 8) form the basis of our analysis that follows.

3 Differential flow induced chemical instability due to crossed fields

To illustrate the above scheme we now resort to the well known reaction-diffusion system, Lengyel-Epstein model for Chlorite-Iodide-Malonic Acid reaction [19,20]. The reaction is made to occur in a gel, polyacrylamide. It is essentially a five-variable model reduced to a two-variable

one noting that the concentrations of all other variables but chlorite and iodide remain more or less constant in time. The time evolution of these two variables viz. I^- and ClO_2^- denoted by $U(t)$ and $V(t)$ respectively, are then given by;

$$U(t)_t = k_1^{'} - k_2^{'}U(t) - 4k_3^{'}\frac{U(t)V(t)}{(\alpha + U(t)^2)} \tag{9}$$

$$V(t)_t = k_2^{'}U(t) - k_3^{'}\frac{U(t)V(t)}{(\alpha + U(t)^2)}. \tag{10}$$

Here k_1', k_2' and k_3' and α are the kinetic constants of the reaction. If we now consider the addition of starch (which actually complexes with iodide) and allow diffusion to occur in all three directions, the system now looks like for $U(x, y, z, t)$ and $V(x, y, z, t)$,

$$U_t = k_1^{'} - k_2^{'}U - 4k_3^{'}\frac{UV}{(\alpha + U^2)} + D_U\nabla^2 U \tag{11}$$

$$(1/\sigma)V_t = k_2^{'}U - k_3^{'}\frac{UV}{(\alpha + U^2)} + D_V\nabla^2 V. \tag{12}$$

The dimensionless parameter σ arises due to the equilibrium between starch and iodide (σ is defined as $\sigma = 1 + S_0\frac{k_1}{k_2}$, k_1, k_2 are the forward and reverse rate constants of the corresponding first order equilibrium reaction between starch and iodide while S_0 is the initial starch concentration). The role of starch is not only to impart coloration to the system but also to make the effective ratio of diffusion coefficients different from the actual value which is close to unity.

In the presence of crossed fields, i.e., electric field along x and magnetic field along y direction the system of equation get modified into (taking $z_u = z_v = -1$)

$$U_t = k_1^{'} - k_2^{'}U - 4k_3^{'}\frac{UV}{(\alpha + U^2)} + D_U\nabla^2 U - |e|(D_u/kT)\overrightarrow{E}.\overrightarrow{\bigtriangledown}U + (|e|D_u/kT)^2\overrightarrow{E}\times\overrightarrow{B}.\overrightarrow{\bigtriangledown}U \tag{13}$$

$$(1/\sigma)V_t = k_2^{'}U - k_3^{'}\frac{UV}{(\alpha + U^2)} + D_V\nabla^2 V - |e|(D_v/kT)\overrightarrow{E}.\overrightarrow{\bigtriangledown}V + (|e|D_v/kT)^2\overrightarrow{E}\times\overrightarrow{B}.\overrightarrow{\bigtriangledown}V. \tag{14}$$

Now we substitute $u = \frac{U}{\sqrt{\alpha}}$, $v = \frac{k_3^{'}V}{k_2^{'}\alpha}$, $x' = x(k_2^{'}/D_u)^{1/2}$, $y' = y(k_2^{'}/D_u)^{1/2}$, $z' = z(k_2^{'}/D_u)^{1/2}$, $t' = k_2^{'}t$, to obtain

$$u_t = a - u - 4uv/(1 + u^2) - \psi u_x + \phi u_z + u_{xx} + u_{yy} + u_{zz} \tag{15}$$

$$(1/\sigma)v_t = [b(u - uv/(1 + u^2))] - d\psi v_x + d^2\phi v_z + d[v_{xx} + v_{yy} + v_{zz}]. \tag{16}$$

Here ψ, ϕ, the electric and magnetic field containing terms are abbreviated as $\psi = E\frac{|e|}{kT}(D_u/k_2')^{1/2}$, $\phi = EB(\frac{|e|}{kT})^2 D_u(k_2'/D_u)^{1/2}$. Furthermore we have put $a = \frac{k_1'}{k_2'\sqrt{\alpha}}$, $b = \frac{k_3'}{k_2'\sqrt{\alpha}}$. Also d is the ratio of the diffusion coefficients ($d = D_v/D_u$) of the activator (ClO_2^-) and inhibitor (I^-). All the quantities $d, a, b, u, v, x', y', z', t'$ as well as ψ and ϕ in equations (15, 16) are dimensionless. (For simplicity, from now onwards we drop the prime ($'$) from x', y', z', t'.)

The fixed point of the dynamical system is given by $u_{ss} = a/5$ and $v_{ss} = 1 + a^2/25$, i.e., the homogeneous steady state is independent of b. This well-known model in absence of field terms has been used for suggesting the reaction dynamics of the first experimentally observed Turing pattern and latter on in many other related issues. An important content of the present work is to extend the model to include the effect of electric and magnetic fields. For a fixed set of experimentally admissible dimensionless parameter values of a, b and d it is possible to vary σ by adjusting the initial concentration of starch, the complexing agent in the Lengyel-Epstein model which plays an important role in determining the stability of various regimes. In absence of diffusion and external fields, the Hopf bifurcation line (b vs. a), below which the system undergoes stable oscillations is given by $b = 3a/5 - 25/a$. The reaction-diffusion system on the other hand in absence of external fields gives rise to Turing bifurcation line if the curve $(3da^2 - 5ab - 125d)^2 = 100abd(25 + a^2)$ is plotted. This curve is independent of σ. The homogeneous steady state is unstable below this line. Thus as one increases σ, the control parameter, the Hopf line shifts downwards and once it crosses the Turing line diffusion-driven instability sets in resulting in initiation of pattern formation under suitable boundary condition [24]. The focal theme of the present investigation is to show that the application of crossed electric and magnetic fields, however, may shift the boundary line below the Hopf curve (for the same σ value for which no instability arises in absence of fields) giving rise to differential flow induced chemical instability and pattern selection.

The crossed field induced instability can be examined by a linear stability analysis of the system (15) and (16). To this end we begin with linearized version of equations (15) and (16) as

$$\partial u_t = f_u\partial u + f_v\partial v - \psi\partial u_x + \phi\partial u_z + \partial u_{xx} + \partial u_{yy} + \partial u_{zz} \tag{17}$$

$$\partial v_t = g_u\partial u + g_v\partial v - d\psi\partial v_x + d^2\phi\partial v_z + d\partial v_{xx} + d\partial v_{yy} + d\partial v_{zz} \tag{18}$$

where $\partial u(= u(x, y, z, t) - u_{ss})$ and $\partial v(= v(x, y, z, t) - v_{ss})$ are small deviations from homogeneous steady state values u_{ss} and v_{ss}, respectively. f_u, f_v, g_u, g_v are the partial derivatives of the reaction terms in (15) and (16), evaluated at the steady state. A closer look into the linearized equations (17) and (18) reveals that a Turing like form of the spatio-temporal perturbation ∂u and ∂v (as $\cos k_x x \cos k_y y \cos k_z z \exp(-\lambda t)$, k_x, k_z and λ being the wave vectors and frequency, respectively) can not work because of the presence of the spatial first derivative terms. However the presence of these terms suggests that they are reminiscent of the differential flow induced terms [26] that occur

for a system involving activator and inhibitor kinetics in a reactive flow resulting in instability. To explore the role of spatially localized perturbation in a similar spirit we take resort to spatial Fourier expansion of the form

$$(\partial u, \partial v) = \frac{1}{2\pi}\int_{-\infty}^{\infty}(\partial u_0(k), \partial v_0(k))\exp(\lambda t + ik_x x + ik_z z) \times \cos k_y y dk_x dk_y dk_z. \quad (19)$$

Here λ satisfies the following relation which is obtained by making use of the said form of the spatio-temporal perturbation

$$\begin{aligned}\lambda^2 &- [f_u - ik_x\psi + ik_z\phi - k_x^2 - k_y^2 + \sigma g_v \\ &- i\sigma k_x d\psi + i\sigma k_z d^2\phi - \sigma d k_x^2 - \sigma d k_y^2 - \sigma d k_z^2]\lambda \\ &+ [f_u - ik_x\psi + ik_z\phi - k_x^2 - k_y^2 - k_z^2][\sigma g_v - i\sigma k_x d\psi \\ &+ i\sigma k_z d^2\phi - \sigma d k_x^2 - \sigma d k_y^2 - \sigma d k_z^2] - \sigma g_u f_v = 0. \quad (20)\end{aligned}$$

The above equation gives the dispersion relation $\lambda = \lambda(k_x, k_y, k_z)$. The equation is too cumbersome to arrive at an explicit analytical condition for instability which is given by $\mathrm{Re}\lambda > 0$. Further this is subject to boundary conditions for the spatio-temporal perturbations required for the linear stability analysis. A physically allowed choice is zero concentration gradient at the boundaries, such that $\frac{\delta\partial u}{\delta\xi} = 0$ at $\xi = 0$ and $\xi = L_\xi$, where ξ is x, y or z. We impose similar boundary conditions for ∂v. To understand this effect it is instructive to consider only two discrete modes for ∂u as illustration instead of the integral (19)

$$\partial u = Ae^{i(k_x x + k_z z)}\cos k_y y + A' e^{i(k'_x x + k'_z z)}\cos k'_y y.$$

The application of the above-mentioned boundary conditions leads to

$$\begin{aligned}\frac{\delta\partial u}{\delta z}\,|_{z=0} &= iAk_z e^{ik_x x} cos k_y y \\ &+ iA'k'_z e^{ik'_x x}\cos k'_y y = 0 \quad (21)\\ \frac{\delta\partial u}{\delta z}\,|_{z=L_z} &= iAk_z e^{ik_x x + ik_z L_z} cos k_y y \\ &+ iA'k'_z e^{ik'_x x + ik'_z L_z}\cos k'_y y = 0. \quad (22)\end{aligned}$$

Multiplying equation (21) by $\exp(ik_z L)$ and on substraction of the resulting equation from (22) we are led to the condition $\tan k_z L_z = \tan k'_z L_z$. This yields the condition $k_z - k'_z = \frac{2n_z\pi}{L_z}$, $n_z = 1, 2, 3\ldots$ Exactly similar condition may be derived for $k_x - k'_x = \frac{2n_x\pi}{L_x}$, $n_x = 1, 2, 3\ldots$ On the other hand for y-direction the application of zero concentration gradient boundary condition leads to $k_y = \frac{n_y\pi}{L_y}$, $n_y = 1, 2, 3\ldots$

Although illustrated for two nodes it is apparent that the above argument can be extended to higher number of modes further to associate discrete numbers corresponding to wave number components and their combinations. Since λ is a function of three variables $\lambda(k_x, k_y, k_z)$ the search for the positivity of λ may be carried out by varying any two of them (say k_x, k_y) for a fixed value of the other (say k_z) in a surface plot. We draw two sets of such surface plots for two different k_z values in Figures 2 and 3. For a suitable choice of the order of k_z we may refer to the condition $k_z - k'_z = \frac{2n_z\pi}{L_z}$ For $L_z = 10$ and lowest n_z ($n_z = 1$) a rough estimate for k_z is approximately of the order of 0.6. Keeping in view of this estimate we then fix k_z in Figures 2 and 3 as $k_z = 0.6$ and 1.2 respectively. A closer look into equation (20) also reveals

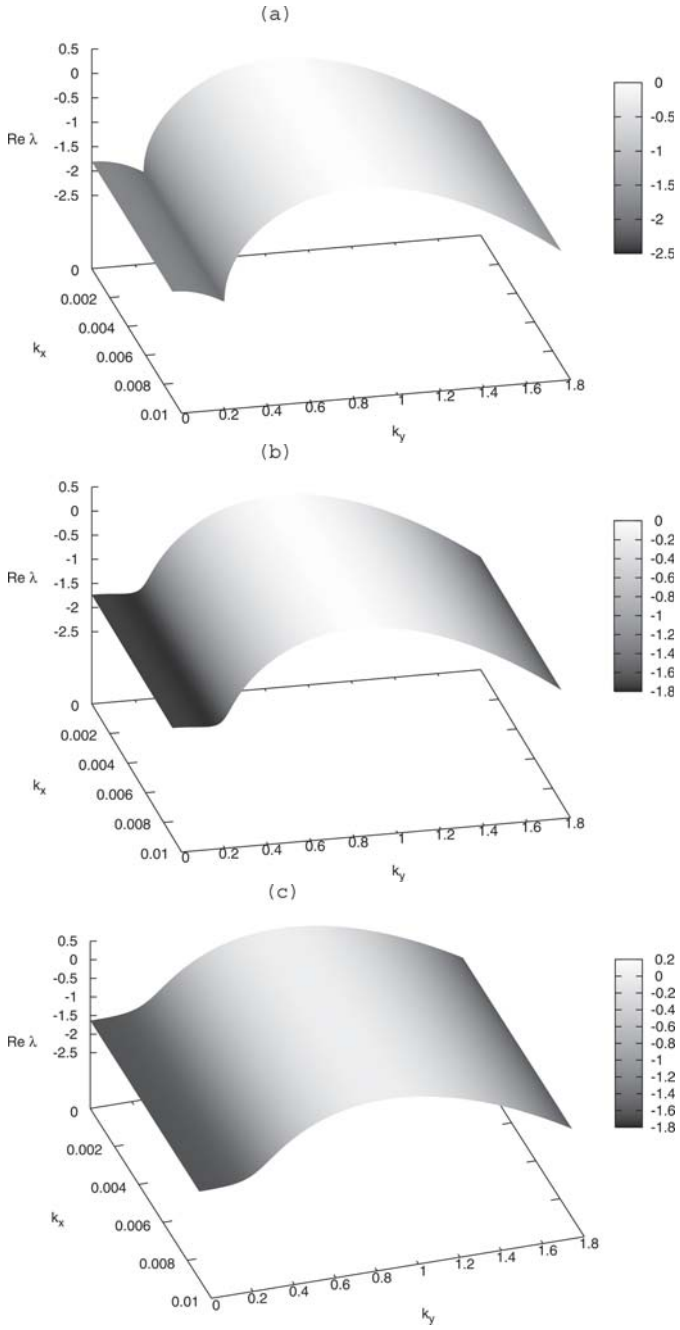

Fig. 2. Dispersion relation: plot of Reλ on $k_x - k_y$ plane for $k_z = 0.6$ for the parameter set $a = 18.0$, $b = 1.5$, $d = 1.6$, $\sigma = 5.9$ for fixed electric field strength ($\psi = 0.01$) applied in the x-direction and varied magnetic field strengths (a) $\phi = 0.0$, (b) $\phi = 0.2$, (c) $\phi = 0.3$ applied in y-direction.

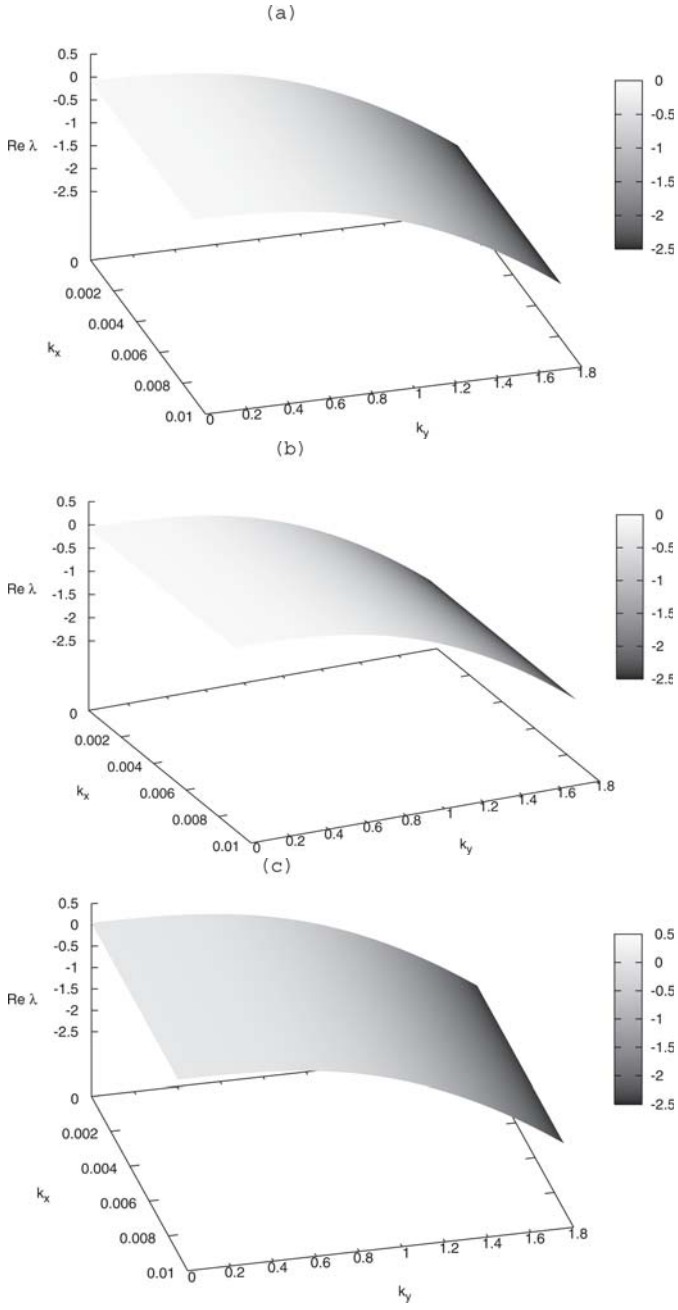

Fig. 3. Dispersion relation: plot of Reλ on $k_x - k_y$ plane for $k_z = 1.2$ for the parameter set $a = 18.0$, $b = 1.5$, $d = 1.6$, $\sigma = 5.9$ for fixed electric field strength ($\psi = 0.01$) applied in the x-direction and varied magnetic field strengths (a) $\phi = 0.0$, (b) $\phi = 0.2$, (c) $\phi = 0.3$ applied in y-direction.

that as k_x and k_z appear either quadratically or in imaginary part, the dispersion curves remain same for the reversal of sign of k_x and k_z. This may also be checked by numerical computation. Thus the positive wave number regions have been plotted in Figures 2 and 3. In Figure 2 we draw three surface plots for the planes Reλ as a function of k_x and k_y for a fixed $k_z = 0.6$, for the parameter set $a = 18.0, b = 1.5, d = 1.6, \sigma = 5.9$ and for a fixed electric field of strength $\psi = 0.01$ applied along x-direction and varied magnetic field strength (a) $\phi = 0.0$, (b) $\phi = 0.2$, (c) $\phi = 0.3$. All the eigenvalues are negative in absence of magnetic field ($\phi = 0.0$). The system however for the same parameter set loses stability beyond $\phi = 0.8$. In Figure 3 the loss of stability occurs at same ϕ(=0.3) when k_z is set at 1.2 and all other parameters are kept same as before. The imaginary parts of λ in all these cases remain vanishingly small (Im$\lambda \sim 0$) which implies the condition for formation of stationary pattern.

4 Numerical simulation and pattern formation

Before going over to full numerical simulations it is necessary to introduce the appropriate boundary conditions for the problem described by equations (15) and (16) involving the differential flow terms due to electric and magnetic fields. In defining the fluxes we take care of the field containing terms as well. Therefore we write for the u-component

$$\begin{aligned} J_x &= \frac{\partial u}{\partial x} - \psi u \\ J_y &= \frac{\partial u}{\partial y} \\ J_z &= \frac{\partial u}{\partial z} + \phi u \end{aligned} \tag{23}$$

and for the v component

$$\begin{aligned} J_x &= d\frac{\partial v}{\partial x} - \psi v \\ J_y &= d\frac{\partial v}{\partial y} \\ J_z &= d\frac{\partial v}{\partial z} + \phi v. \end{aligned} \tag{24}$$

The flux along x-derivative is not zero since in reality the ionic species move in and out because of the electric field. At the boundary the concentration gradients (not the fluxes) are therefore taken to be zero. This condition is also consistent with the form of spatio-temporal perturbation used in our linear stability analysis.

The computations were performed using equations (15) and (16) by explicit Euler method on a three dimensional grid $200 \times 200 \times 10$ with $\triangle x = \triangle y = 1.0$, $\triangle z = 1.0$ and time step $\triangle t = 0.0005$ and with zero flux (concentration) boundary conditions. The parameter set used allows the system to stay in the Hopf region for $\sigma = 5.9$ and the system remains homogeneous. The simulations were started with spatially random perturbation of 1% around the steady state. As the constant external electric field (dimensionless value $\psi = 0.01$) is applied along positive x-direction one observes (Fig. 4) an inhomogeneous spatial structure in the form of stationary spots only when a magnetic field over a certain strength along positive y-direction is applied simultaneously in the reaction plane. Our numerical simulation shows that for the given value of electric field

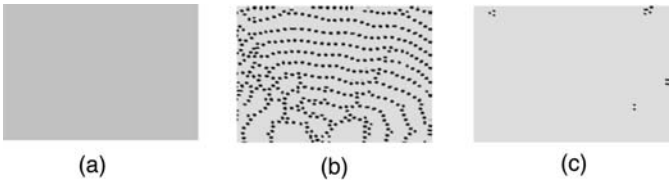

Fig. 4. Magnetic field induced transition of Hopf instability to Turing instability: numerically simulated (in three dimensions) spatial pattern in CIMA system for $a = 18.0$, $b = 1.5$, $d = 1.6$, $\sigma = 5.9$ (grid size $200 \times 200 \times 10$ with $\triangle x = \triangle y = 1.0$, $\triangle z = 1.0$). Bright pixels represent high ClO_2^- concentration. (a) $\phi = 0.0$, (b) $\phi = 0.2$, (c) $\phi = 0.3$. The electric field ($\psi = 0.01$) is applied in the reaction plane along x-direction and magnetic field in the same plane along y-direction is varied.

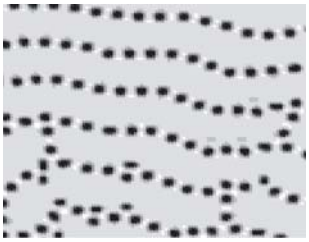

Fig. 5. An enlarged picture of a small area (50×50) taken from the net 200×200 area shown in Figure 3b.

strength the spatial inhomogeneity appears only beyond a critical magnetic field strength (dimensionless value higher than $\phi = 0.2$). A typical magnetic field induced pattern is drawn in Figure 4b for $\phi = 0.2$. A comparison between linear stability analysis and numerical simulation in terms of the observed wavenumbers seems pertinent. It appears from Figure 3c that instability should appear at k_y close to zero. A look into Figure 4 clearly reveals that a distinct wave number can be associated with the numerically simulated pattern. As pointed out earlier the application of zero concentration gradient boundary condition on the spatiotemporal perturbation in the linear stability analysis yields $k_y^2 = \frac{n_y^2 \pi^2}{L_y^2}$. For around ten nodes in the y direction (Fig. 5), $n_y = 10$ and $L_y = 200$, k_y is approximately 0.15 which corroborates with the linear stability analysis. An enlarged version of the selected area of Figure 4b is shown in Figure 5. The stable structure tends to vanish at higher strengths of the magnetic field as shown in Figure 4c.

It is also instructive to look at the role of diffusion along z-direction in the context of cross-field induced effects we are studying. This has been illustrated in Figure 6 where we have displayed the variation of concentration along this direction at two different sites of the xy-plane. The diffusional flux along z is a consequence of Lorentz force acting on the ionic species in the reaction system. It also follows from Figure 6 and our numerical experience that the qualitative nature of variation of concentration along z remains the same regardless of the specificity of the site of the xy reaction plane.

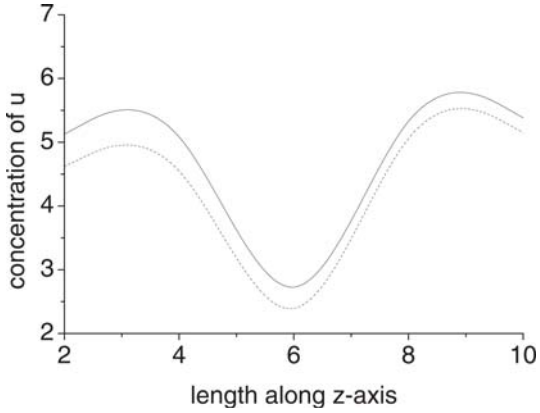

Fig. 6. The variation of concentration of u along z-axis at two different sites of the xy plane (50, 50, continuous line) and (2.5, 2.5, dotted line).

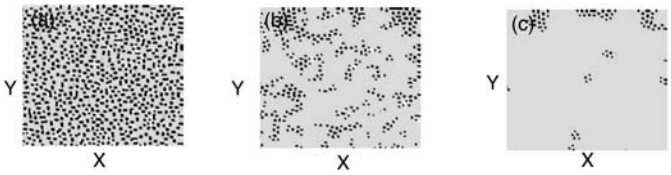

Fig. 7. Numerically simulated (in three dimensions) field distorted Turing pattern for $a = 18.0$, $b = 1.5$, $d = 1.6$, $\sigma = 7.0$ (grid size $200 \times 200 \times 10$ with $\triangle x = \triangle y = 1.0, \triangle z = 1.0$). Bright pixels represent high concentration of ClO_2^- for (a) $\psi = 0.0$, $\phi = 0.0$; (b) $\psi = 0.01$, $\phi = 0.3$; (c) $\psi = 0.01$, $\phi = 0.4$ (the electric field (ψ) being applied in the reaction plane along x-direction and magnetic field (ϕ) in the same plane along y-direction).

Our numerical experience shows that beyond a certain thickness of the reaction plane the system tends to be homogeneous. It is therefore apparent that although the activator and the inhibitor ions are diamagnetic in character, the magnetic field in reaction-diffusion system in addition to the diffusional flux along the direction of charge separation plays an important role in pattern formation and selection. We emphasize that the shift of the stability boundary in generating spatial structure due to differential flow by application of magnetic field is different from the scenario that leads to Turing pattern. To illustrate we now consider the following situation. For $\sigma = 7.0$ the reaction-diffusion system in absence of the applied fields exhibits the usual Turing pattern in the form of spots as shown in Figure 7a. Application of the electric and the magnetic fields ($\psi = 0.01$ and $\phi = 0.2$) results in deformation of pattern (Fig. 7b). As the electric field strength is kept constant and the magnetic field is increased one observes greater distortion of pattern (Fig. 7c). Thus the scenarios depicted in Figure 4 illustrating the pattern formation due to differential flow induced instability and those in Figure 7 displaying the modification of Turing pattern by crossed fields are generically distinct

Before closing this section a few points regarding the observability of the effect in chlorine dioxide-iodide-malonic acid system seems pertinent. To meet the condition of the cross-field effect the reaction plane should be thin but at the same time must allow a perceptible separation of the charges along z-direction. Since the effect of electric field on Turing Pattern in this system has already been an aspect of experimental study it is worthwhile to look for the effect by simultaneously applying the magnetic field with implementation of such a set-up [12]. The required magnitude of the electric and magnetic field strength E and B may be estimated in actual terms from the dimensionless expressions $\psi = \frac{E|e|}{kT}(\frac{D_u}{k_2'})^{1/2} = \frac{EF}{RT}(D_u/k_2')^{1/2}$ and $\phi = EB(\frac{|e|}{kT})^2 D_u(k_2'/D_u)^{1/2} = EB(\frac{\mathbf{F}}{RT})^2 D_u(D_u/k_2')^{-1/2}$ where k_2' is expressed as k_2 times initial concentration of ClO_2,$[ClO_2]_0$. Putting $k_2 = 6 \times 10^3$ mole^{-1} lit s^{-1}, $[ClO_2]_0 = (1/6) \times 10^{-3}$ moles/lit and $D_{ClO_2}(=D_u) = 1 \times 10^{-5}$ cm^2/s, one requires the electric field E as 0.06 Volt/cm to correspond $\psi = 0.01$ and magnetic field B as 60 Gauss to correspond $\phi = 0.1$ at temperature 25 °C to realize a typical pattern induced by crossed-fields.

5 Conclusion

In conclusion, we consider a reaction-diffusion system in crossed electric and magnetic fields. It is shown that a charge separation of the reacting species across the reaction plane may result in differential flow induced chemical instability and a spatial inhomogeneity on a homogeneous stable state resulting in pattern formation. The distinctive role of magnetic field in creating spatial inhomogeneity even when the reacting species are not paramagnetic is thus immediately apparent. The situation is different from those pertaining to the control of traveling waves by magnetic fields where one considers paramagnetic reacting species. We hope that the present formulation of reaction-diffusion system in electro-magnetic fields will be useful for further investigation from theoretical as well as from experimental point of view.

Thanks are due to the CSIR, Government of India, for partial financial support (S.S.R. and S.K.).

References

1. I.R. Epstein, J.A. Pojman, *An Introduction to Nonlinear ChemicalDynamics* (Oxford University Press, New York, 1998)
2. J.D. Murray, *Asymptotic Analysis* (Springer-Verlag, New York, 1984)
3. A.M. Turing, Philos. Trans. R. Soc. London **327**, 37 (1952)
4. J.R. Bamforth, S. Kalliadasis, J.H. Merkin, S.K. Scott, Phys. Chem. Chem. Phys. **2**, 4013 (2000)
5. S. Schmidt, P. Ortoleva, J. Chem. Phys. **71**, 1010 (1979)
6. S. Schmidt, P. Ortoleva, J. Chem.Phys. **74**, 4488 (1981)
7. A. Toth, D. Horvath, W.V. Saarloos, J. Chem. Phys. **111**, 10964 (1999)
8. B.Z. Virany, A. Szommer, A. Toth, D. Horvath, Phys. Chem. Chem. Phys. **6**, 3396 (2004)
9. J. Krempasky, M. Smrcinova, Collect. Czehc. Chem. Commun. **54**, 1232 (1989)
10. S.S. Riaz, S. Kar, D.S. Ray, Physica D **203**, 224 (2005)
11. S.S. Riaz, S. Kar, D.S. Ray, J. Chem. Phys. **121**, 5395 (2004)
12. B. Schmidt, P. De Kepper, S.C. Müller, Phys. Rev. Lett. **90**, 118302 (2003)
13. E. Steiner, T. Ulrich, Chem. Rev. **89**, 51 (1989)
14. K. Bhattacharyya, M. Chowdhury, Chem. Rev. **93**, 507 (1993)
15. M. Halder, P.P. Parui, K.R. Gopidas, D.N. Nath, M. Chowdhury, J. Phys. Chem. A **106**, 2200 (2002)
16. E. Boga, Kadar, G. Peintler, I. Nagypal, Nature **347**, 749 (1990)
17. X He, K. Kustin, I. Nagypal, G. Peintler, Inorg. Chem. **33**, 2077 (1994)
18. J.D. Lechleiter, D.E. Clapham, Cell **69**, 283 (1992)
19. I. Lengyel, I.R. Epstein, Science **251**, 650 (1991)
20. V. Castets, E. Dulos, J. Boissonade, P. De Kepper, Phys. Rev. Lett. **64**, 2953 (1990)
21. M. Menzinger, A.B. Rovinsky, in *Chemical Waves and Patterns*, edited by R. Kapral, K. Showalter (Kluwer, Dordrecht), pp. 365–397
22. H. Sevcikova, M. Marek, Physica D **9**, 140 (1983)
23. H. Sevcikova, M. Marek, Physica D **21**, 61 (1986)
24. O. Jensen, V.O. Pannbacker, E. Mosekilde, G. Dewel, P. Borckmans, Phys. Rev. E **50**, 736 (1994)
25. A.F. Munster, F. Hasal, D. Smita, M. Marek, Phys. Rev. E **50**, 546 (1994)
26. A.B. Rovinsky, M Menzinger, Phys. Rev. Lett. **69**, 1193 (1992)